

# Response-based estimation of sea state parameters—influence of filtering

Ulrik Dam Nielsen\*

*Department of Mechanical Engineering, Technical University of Denmark, DK-2800 Lyngby, Denmark*

Received 21 November 2006; accepted 8 March 2007

Available online 15 March 2007

## Abstract

Reliable estimation of the on-site sea state parameters is essential to decision support systems for safe navigation of ships. The wave spectrum can be estimated from procedures based on measured ship responses. The paper deals with two procedures—Bayesian Modelling and Parametric Modelling—which both use complex-valued frequency response functions (FRF) to estimate the wave spectrum. It is therefore interesting to investigate how the filtering aspect, introduced by FRF, affects the final outcome of the estimation procedures. In order to do this, extensive numerical simulations—with known wave parameters—are carried out for a large container vessel. The study shows that filtering has an influence on the estimations, since high-frequency components of the wave excitations are not estimated as accurately as lower frequency components.

© 2007 Elsevier Ltd. All rights reserved.

*Keywords:* Sea state parameters; Wave spectra; Measured ship responses; Bayesian modelling; Parametric modelling; Filtering

## 1. Introduction

### 1.1. Decision support systems

Decision support systems based on in-service monitoring systems can be applied to increase the operational safety of ships, e.g. [Huss and Olander \(1994\)](#) and [Nielsen \(2004\)](#). The on-site sea state is paramount for the decision support system to give reliable guidance. The literature contains several studies on the estimation of (directional) wave spectra based on measured ship responses. Conceptually, two methods are considered: (1) Parametric Modelling which assumes the wave spectrum to be composed of parameterised wave spectra, so that the underlying wave parameters are sought for from an optimisation, e.g. [Tannuri et al. \(2003\)](#), [Aschehoug \(2003\)](#) and [Nielsen \(2006\)](#), or (2) Bayesian Modelling where the directional wave spectrum is found directly as the values in a completely discretised frequency-directional domain, e.g. [Iseki and Terada \(2002\)](#), [Waals et al. \(2002\)](#) and [Nielsen](#)

(2006). In general, the methods are based on linear spectral analysis which assumes a linear relationship between the wave excitations and the ship responses. This assumption facilitates the use of complex-valued frequency response functions established by measurements, closed-form (analytical) expressions, strip theories or three-dimensional time domain codes.

### 1.2. Background

Independently of the calculation procedure, the use of complex-valued frequency response functions introduces, or illustrates, the aspect of filtering, which means that ship responses, in general, are only sensitive to wave excitations characterised by wave lengths in a certain interval, e.g. [Pascoal et al. \(2005\)](#) and [Tannuri et al. \(2003\)](#). In the view of response-based estimation of wave spectra, this means that a model, in principle, cannot predict values of components in the entire frequency band of a wave spectrum. Therefore, the estimations will always be characterised by some uncertainty, no matter how accurate the hydrodynamic behaviour of the ship is described by the complex-valued frequency response functions.

\*Tel.: +45 4525 1970; fax: +45 4588 4325.

E-mail address: [udn@mek.dtu.dk](mailto:udn@mek.dtu.dk).

### 1.3. The study

This paper contains an extensive study of numerical simulations of time histories with an overall focus on the estimation of sea state parameters. Thus, a large amount of wave estimations are carried out from numerical simulations, with exact known underlying wave excitations, i.e. wave spectrum parameters. In this way it is possible to evaluate the influence of the filtering aspect on the estimation model, given that the hydrodynamic model of the ship is known to be exact and, hence, give a perfect relationship between the wave excitations and the ship responses for the specific ship. Similar studies, although not as comprehensive, have been carried out by Nielsen (2006), Pascoal et al. (2005) and Tannuri et al. (2003), where the two latter studies, however, did not consider the problem of a ship being underway, i.e. the speed-of-advance problem first dealt with by Iseki and Ohtsu (2000). Moreover, the present paper compares the results of the Bayesian Modelling with those of the Parametric Modelling.

### 1.4. Sea state estimations from measured ship responses

Today, means of obtaining estimations of the sea state parameters exist. Such means include moored wave rider buoys and current meters, satellite measurements and wave radar systems. The latter two of these means do not suffer from the problems related to the fixed position of a moored buoy and current meters, but do, on the other hand, require complex computational hardware and have a high initial cost, cf. Tannuri et al. (2003), not to mention calibration and maintenance. For this reason it is of interest to be able to estimate the wave spectrum from measured ship responses, which are easily accessible—and, as a matter of fact, already at hand—from the sensor measurements done in an in-service monitoring system. In this way, the ship is itself to be considered as a kind of wave buoy. It is, however, important to keep in mind that wave estimations carried out from measured ship responses cannot be expected to be as accurate as the wave estimations from a real wave buoy; primarily due to filtering introduced by the (high) inertia of a ship hull (with a complex geometry) as compared to the relatively small size and well-described geometry of a wave buoy. Secondly, the wave estimations from ship responses cannot be expected as accurately as the estimations from a real wave buoy, since a ship, in general, is moving with a forward speed when the estimations are carried out. In the comparisons presented later these issues should be kept in mind, since some of the statements and conclusions reflect that the wave estimations are *ship response-based*.

### 1.5. Composition of paper

The organisation of the paper is as follows. In the next section the fundamental theory of Bayesian Modelling and

Parametric Modelling is outlined. In addition, the section contains a subsection that describes how the numerical simulation of the ship responses is conducted. The third section sets up the numerical study which will be carried out. Thus, a number of test cases are organised and the specific ship and the considered motion responses are described. Moreover, the section lists the integrated wave parameters, on which comparisons can be made. The results of the study are given in the fourth section; primarily in tabular form and visualised graphically. Finally, the last section draws conclusions from the presented material.

## 2. Theory

### 2.1. Bayesian Modelling

This subsection gives the fundamentals of Bayesian Modelling applied to estimate directional wave spectra. The subsection is by no means comprehensive and the literature should be consulted for details, e.g. Iseki and Terada (2002), Nielsen (2006, 2007).

On the assumption that the ship responses are stationary and linear with the incident waves, the complex-valued frequency response functions  $\Phi_i(\omega_e, \beta)$  and  $\Phi_j(\omega_e, \beta)$  for the  $i$ th and  $j$ th responses yield the theoretical relationship between the  $i$ th and the  $j$ th components of the cross spectra  $S_{ij}(\omega_e)$  and the directional wave spectrum  $E(\omega_e, \beta)$  through the following integral equation:

$$S_{ij}(\omega_e) = \int_{-\pi}^{\pi} \Phi_i(\omega_e, \beta) \overline{\Phi_j(\omega_e, \beta)} E(\omega_e, \beta) d\beta, \quad (2.1)$$

where the bar denotes the complex conjugate, and with  $\beta$  being the heading of the ship (relative to the waves) and  $\omega_e$  being the encounter frequency. The heading is defined so that  $\beta = \pi$  corresponds to head waves. It should be realised that the wave spectrum is given in terms of the heading, which is justified by letting the wave direction and the course of the ship be given relative to the same datum, so that the heading and the wave direction are coincident. Finally, it should be noted that the complex-valued frequency response functions are written as functions of only the heading and the encounter frequency, since the implication of changing of other operational parameters is understood.

The wave spectrum is advantageously estimated in the wave frequency domain. This means that the speed-of-advance, or triple-valued function, problem needs to be considered. This problem has been properly incorporated by Iseki and Ohtsu (2000), for details see Nielsen (2006).

In terms of matrix notation, (2.1) can be written as

$$\mathbf{b} = \mathbf{A}\mathbf{f}(\mathbf{x}) + \mathbf{w}. \quad (2.2)$$

The vector function  $\mathbf{f}(\mathbf{x})$  expresses the unknown values of the wave spectrum  $E(\omega, \beta)$  through a non-negativity constraint  $\mathbf{f}(\mathbf{x}) = \exp(\mathbf{x})$ , so that  $\mathbf{x} = \ln E(\omega, \beta)$ . The vector  $\mathbf{w}$  is a Gaussian white noise sequence vector with zero mean

and variance  $\sigma^2$ , introduced for stochastic reasons so that the Bayesian modelling is facilitated, cf. Akaike (1980). The vector  $\mathbf{b}$  contains the elements of  $S_{ij}(\omega_e)$ , and the coefficient matrix  $\mathbf{A}$  has elements according to the products of the transfer functions and the derivative of the wave frequency, cf. Eq. (2.1).

In principle, (2.2) can be solved for  $\mathbf{x}$  by minimising  $\chi^2(\mathbf{x})$  with

$$\chi^2(\mathbf{x}) \equiv \|\mathbf{A}\mathbf{f}(\mathbf{x}) - \mathbf{b}\|^2, \quad (2.3)$$

where  $\|\cdot\|$  represents the  $L_2$  norm.

The equation system given by (2.3) is in most cases underdetermined, or otherwise degenerate, which means that the solution is unstable. To overcome this problem Bayesian Modelling is introduced, see Akaike (1980). As will be shown in the following, it is possible to evaluate  $\mathbf{x}$  by maximisation of the product of the likelihood function and the prior distributions, which must be defined properly. The prior distributions act as a stochastic constraint and are a general character of the model which is known in advance, e.g. Iseki and Terada (2002). For the model above, the likelihood function is written as

$$l(\mathbf{x}|\sigma^2) = \left(\frac{1}{2\pi\sigma^2}\right)^{P/2} \exp\left(-\frac{1}{2\sigma^2}\|\mathbf{A}\mathbf{f}(\mathbf{x}) - \mathbf{b}\|^2\right), \quad (2.4)$$

where  $P$  is the total number of integral equations derived from (2.1) including a number of equations yielding equivalence of energy on the left- and right-hand side of (2.1), cf. Nielsen (2006).

In this paper, two prior distributions are taken into account, cf. Nielsen (2007). Both distributions are a Gaussian smoothness prior distribution which minimises the sum of the second order difference of the unknown vector  $\mathbf{x}$  in order to smoothen the change with frequency and direction, respectively, of the wave spectrum, e.g. Nielsen (2006) and Iseki and Terada (2002). The prior distributions are therefore defined by the minimisation of the functionals

$$\sum_{n=1}^N \sum_{m=1}^M \varepsilon_{1mn}^2 = \sum_{n=1}^N \sum_{m=1}^M (x_{m-1,n} - 2x_{m,n} + x_{m+1,n})^2, \quad (2.5)$$

$(x_{0,n} = x_{M,n}, \quad x_{M+1,n} = x_{1,n}),$

$$\sum_{n=1}^N \sum_{m=1}^M \varepsilon_{2mn}^2 = \sum_{m=1}^M \sum_{n=2}^{N-1} (x_{m,n-1} - 2x_{m,n} + x_{m,n+1})^2, \quad (2.6)$$

where  $N$  and  $M$  are the number of discrete wave frequencies and discrete headings, respectively. Thus, considering  $\varepsilon_{1mn}$  and  $\varepsilon_{2mn}$  to be normal distributions with zero mean and variance  $\sigma^2/u^2$  and  $\sigma^2/v^2$ , respectively, the prior distribution is given in terms of the so-called hyperparameters  $u$  and  $v$ . In matrix notation the functionals can be written as, see e.g. Press et al. (1992),

$$\sum_{n=1}^N \sum_{m=1}^M \varepsilon_{1mn}^2 = \mathbf{x}^T \mathbf{H}_1 \mathbf{x}, \quad (2.7)$$

$$\sum_{n=1}^N \sum_{m=1}^M \varepsilon_{2mn}^2 = \mathbf{x}^T \mathbf{H}_2 \mathbf{x}. \quad (2.8)$$

In accordance with Akaike (1980), the posterior distribution  $p(\mathbf{x}|u, v, \sigma^2)$  is proportional to the product of the likelihood function and the prior distribution, which can be written as, see Nielsen (2007),

$$p(\mathbf{x}|u, v, \sigma^2) = c \left(\frac{1}{2\pi\sigma^2}\right)^{(P+KM)/2} |\det(u^2\mathbf{H}_1 + v^2\mathbf{H}_2)|^{1/2} \times \exp\left(-\frac{1}{2\sigma^2}S(\mathbf{x})\right) \quad (2.9)$$

with

$$S(\mathbf{x}) = \|\mathbf{A}\mathbf{f}(\mathbf{x}) - \mathbf{b}\|^2 + \mathbf{x}^T(u^2\mathbf{H}_1 + v^2\mathbf{H}_2)\mathbf{x} \quad (2.10)$$

and where  $c$  is a normalising factor independent of the model parameters  $\mathbf{x}$  and the hyperparameters  $u$  and  $v$ .

The hyperparameters control the trade-off between the good-fit of the solution to the data (i.e. agreement between solution and data) and the smoothness, or stability, of the solution, and the optimum values of the hyperparameters are determined by minimising the control criterion ABIC, cf. Akaike (1980) and Nielsen (2007),

$$\text{ABIC} = -2 \ln \int p(\mathbf{x}|u, v, \sigma^2) d\mathbf{x} \quad (2.11)$$

## 2.2. Parametric Modelling

Parameterised wave spectra, e.g. Goda (2000), are typically considered reliable for describing the variation with frequency of ocean wave spectra. Moreover, the angular spread of wave spectra can be described by certain parameters, e.g. Longuet-Higgins et al. (1961) and Goda (2000). In the following the estimation method based on Parametric Modelling will be outlined briefly. Details can be found in the literature, e.g. Nielsen (2006) and Tannuri et al. (2003).

The governing equation system which facilitates Parametric Modelling is derived in the previous subsection as Eq. (2.3). Hence, Parametric Modelling aims at minimising (2.3), which means that the solution is obtained by

$$\min \|\mathbf{A}\mathbf{f}(\mathbf{x}) - \mathbf{b}\|^2. \quad (2.12)$$

As input,  $\mathbf{f}(\mathbf{x})$ , to this equation system, the following 10-parameter bimodal spectrum is considered, e.g. Tannuri et al. (2003) and Hogben and Cobb (1986)

$$E(\omega, \theta) = \frac{1}{4} \sum_{i=1}^2 \frac{(((4\lambda_i + 1)/4)\omega_{p,i}^4)^{\lambda_i}}{\Gamma(\lambda_i)} \frac{H_{s,i}^2}{\omega^{4\lambda_i+1}} A(s_i) \times \cos^{2s_i} \left( \frac{\theta - \theta_{\text{mean},i}}{2} \right) \exp \left[ -\frac{4\lambda_i + 1}{4} \left( \frac{\omega_{p,i}}{\omega} \right)^4 \right] \quad (2.13)$$

with  $H_s$  being the significant wave height,  $\lambda$  is the shape parameter of the spectrum,  $\theta_{\text{mean}}$  is the mean wave

direction,  $\omega_p$  is the angular peak frequency, and  $s$  represents the spreading parameter.

$$A(s) = \frac{2^{2s-1} \Gamma^2(s+1)}{\pi \Gamma(2s+1)} \quad (2.14)$$

is a constant introduced to normalise the area under the  $\cos^{2s}$  curve and  $\Gamma$  denotes the Gamma function.

The wave spectrum expressed by (2.13) considers basically a sea component ( $i = 1$ ) and a swell component ( $i = 2$ ), and on this basis it is, in theory, possible to model most ocean wave spectra, e.g. Hogben and Cobb (1986). The solution of equation (2.12) implies a non-linear optimisation problem from which the best-fit-values can be determined. Hence, the final outcome of the Parametric Modelling is constituted by the parameters

$$\{H_{s,1} \ \lambda_1 \ \theta_1 \ \omega_{p,1} \ s_1 \ H_{s,2} \ \lambda_2 \ \theta_2 \ \omega_{p,2} \ s_2\}. \quad (2.15)$$

### 2.3. Cross spectral analysis

It should be noted that the cross spectral analysis of the responses is carried out by use of multivariate autoregressive modelling, e.g. Akaike and Nakagawa (1988), by application of the so-called stepwise least squares algorithm, see Neumaier and Schneider (2001), for the determination of the MAR coefficients. Detailed information can be found in Nielsen (2005).

### 2.4. Numerical simulation of responses

Ship motions can, in principle, be found by a time domain solution

$$\boldsymbol{\eta} = \boldsymbol{\eta}(t) \quad (2.16)$$

of the generalised equations of motion where the motions, in six degrees of freedom  $\boldsymbol{\eta} = [\eta_1, \eta_2, \eta_3, \eta_4, \eta_5, \eta_6]^T$ , are the surge, sway, heave, roll, pitch, and the yaw. In addition, global ship responses, e.g. the vertical acceleration and the wave induced bending moment, can be derived from the ship motions. In the following, a general global ship response  $R(t)$  will be considered, without differentiation between ship motions and derived responses.

On the assumption of a linear relationship between responses and wave excitations, the time domain solution of the response  $R(t)$  of a ship can be expressed in terms of the complex-valued frequency response function  $\Phi_R(\omega, \beta)$ , see for example Denis and Pierson (1953). In this paper, the time domain solution of the response is, however, presented with the same format as in Jensen and Capul (2006) and Jensen and Pedersen (2006), although the latter references consider only unidirectional waves. Thus, the response is written as a Gaussian process introduced by the set of uncorrelated, standard normal distributed variables  $u_{mn}$  and  $\bar{u}_{mn}$ . Hence,

$$R(t) = \sum_{n=1}^{N_0} \sum_{m=1}^{M_0} [u_{mn} c_{mn}(t) + \bar{u}_{mn} \bar{c}_{mn}(t)]. \quad (2.17)$$

The deterministic coefficients  $c_{mn}(t)$  and  $\bar{c}_{mn}(t)$  are given by

$$\begin{aligned} c_{mn}(t) &= \sigma_{mn} |\Phi_R(\omega_n, \beta_m)| \cos(\omega_{e,n} t + \varepsilon_{mn}), \\ \bar{c}_{mn}(t) &= -\sigma_{mn} |\Phi_R(\omega_n, \beta_m)| \sin(\omega_{e,n} t + \varepsilon_{mn}), \\ \sigma_{mn}^2 &= E(\omega_n, \beta_m) \Delta \omega_n \Delta \beta_m, \end{aligned} \quad (2.18)$$

where it should be noted that the discretised number of wave frequencies  $N_0$  and the discretised number of headings  $M_0$  not (necessarily) take the same numbers as in the estimation analysis, cf. Eqs. (2.5) and (2.6). Furthermore, it should be realised that the variation over time is expressed in terms of the encounter frequency

$$\omega_e = \omega - \omega^2 A, \quad A = \frac{V}{g} \cos \beta \quad (2.19)$$

with  $V$  being the speed of the ship, and  $g$  the acceleration of gravity.  $E(\omega_n, \beta_m)$  is the directional wave spectrum under the assumption that the wave direction is measured relative to the ship course (i.e.  $\beta = \theta$ ), and  $\Delta \omega_n$  and  $\Delta \beta_m$  are the increments of the discrete wave frequencies and the discrete headings, respectively. The phase angles are calculated from

$$\varepsilon_{mn} = \frac{\text{Im}[\Phi_R(\omega_n, \beta_m)]}{\text{Re}[\Phi_R(\omega_n, \beta_m)]}. \quad (2.20)$$

It should be noted that for an equidistant frequency discretisation, the signal  $R(t)$  will repeat itself after a period of  $2\pi/\Delta\omega$ . Thus, in order to avoid this problem, the frequency discretisation is taken to be non-equidistant

$$\omega_{i+1} = \omega_i + c \cdot p_i \quad (2.21)$$

with  $c$  as an ‘appropriately’ small factor while  $p_i$  denotes a stochastic variable with values between 0 and 1.

Furthermore, it should be realised that the present simulation technique, similar to that by Jensen and Capul (2006), yields a wave height which varies statistically, e.g. Goda (2000). In particular, this means that any wave record (i.e.  $|\Phi(\omega, \theta)| \equiv 1$ ) has a significant wave height which, in most cases, is not exactly equal to the  $H_s$  applied to the wave spectrum.

### 2.5. Partitioning of directional wave spectra

It is difficult to compare bimodal or, in general, multi-peaked directional wave spectra and it may lead to ambiguous results if the entire spectrum is treated as one wave system. However, it is possible to construct an algorithm which partitions the wave spectrum into components which represent different wave systems, e.g. Komen et al. (1994) and Gerling (1992). The idea is similar to that used in hydrology, cf. Komen et al. (1994), where a topographical domain is decomposed into a set of catchment areas associated with local minima of the topography. The catchment area of a local topography minimum is defined as the area which drains into the minimum point. In analogy, the spectral wave system associated with a given peak of the wave spectrum is defined as the catchment area of the local minimum corresponding to the inverted peak of

the inverted spectral topography. Thus, the domain of a wave system associated with a given spectral peak consists of all spectral points whose paths of steepest ascent lead to that peak. In this sense, a path of steepest ascent is defined on a discretised grid as the direct set of line segments connecting spectral grid points to the highest of the four nearest-neighbour grid points. Hence, Komen et al. (1994) constructs—mathematically (and numerically)—the domain of a wave system by the induction rule which says that “a grid point and its highest nearest-neighbour grid point (if it is higher than the first grid point—otherwise the first grid point is peak) belong to the same wave system”.

The algorithm for partitioning of wave spectra is an extensive study in its own right and will not be treated in detail here. In the analysis, which follows, the code developed by Aarnes and Krogstad (2001) is applied to partition the wave spectrum when bimodal wave spectra are considered. The literature should be consulted for reference, e.g. Gerling (1992) and Komen et al. (1994).

### 3. Numerical study

#### 3.1. Setup of simulations

This section serves to describe the setup of the numerical study which is to be conducted. Thus, the numerical study will be carried out for a container ship with main dimensions as seen in Table 1. The complex-valued frequency response functions of the ship have been calculated by the three-dimensional time domain code WASIM, e.g. the User Manual of WASIM (DNV, 2005). In all the cases, which will be examined, three responses are considered. The responses are the sway, the heave and the pitch motions, and the speed of the vessel is  $V = 10.0$  m/s in all the numerical simulations. It should be realised that the sway response is an asymmetric response with respect to waves entering the starboard/port side, cf. Nielsen (2006) and Tannuri et al. (2003) which discuss also general aspects on responses to include in response-based estimation of wave spectra.

The wave excitations, applied in the numerical simulation of the motion measurements, are based on the wave spectrum given by Eq. (2.13). The wave spectrum is introduced in three fundamental ways: in the first two ways, a unimodal Pierson Moskowitz (i.e.  $\lambda = 1$ ) wave spectrum with only one peak is assumed, whereas a

Table 2

The underlying wave parameters of the test cases and the corresponding speed of the vessel

Case	$H_s$ (m)	$T_p$ (s)	$s$	$\theta$ (deg.)	$V$ (m/s)
A,B,C,D	3.0	8.0	3.0	015,105,180,225	10.0
E,F,G,H	2.0	14.0	4.0	015,105,180,225	10.0
I	3.0/2.0	8.0/14.0	3.0/4.0	015/225	10.0
J	3.0/2.0	8.0/14.0	3.0/4.0	180/225	10.0
K	3.0/2.0	8.0/14.0	3.0/4.0	105/105	10.0

bimodal Pierson Moskowitz wave spectrum with two peaks is considered in the third way. The different fundamental setups are divided into a number of cases, characterised by different wave directions. Thus, the test cases are summarised in Table 2, where it is seen that Cases A–D correspond to wind sea, all with a significant wave height  $H_s = 3.0$  m, a peak period  $T_p = 8.0$  s, and a spreading parameter  $s = 3.0$ , but with different mean wave directions  $\theta = 015^\circ, 105^\circ, 180^\circ$ , and  $225^\circ$ . Cases E–F represent swells with  $H_s = 2.0$  m,  $T_p = 14.0$  s, and  $s = 4.0$ , and with the same variation in wave directions as the wind sea. Finally, Cases I, J and K are the bimodal cases, each being a combination of wind sea and swells having an energy content represented by  $H_s = 3.0$  m and  $H_s = 2.0$  m, respectively. Similarly, the peak period, the spreading parameter and the shape parameter are identical for the individual components of the combined cases to the unimodal cases representing wind sea and swells. The wave directions do, however, vary, so that the first number gives the direction of the wind sea, whereas the second number gives the direction of the swells. It is seen that Case K represents wind sea and swells from the same direction  $\theta = 105^\circ$ .

In the numerical analysis which follows in the next section, each of the cases listed in Table 2 is applied to simulate 20 runs of the set of responses (sway, heave, pitch) mentioned above, so that a total of 220 simulations are made. All the runs have a duration of 15 min corresponding to 900 s. Furthermore, it should be noted that no white noise has been added to the numerical generated time series and, similar, no uncertainties are considered in the estimations, so that the used complex-valued frequency response functions are assumed to give a perfect description of the hydrodynamic behaviour of the ship. The discretisation of the wave field used in the simulations, cf. Eq. (2.17), is based on a constant number of headings  $M_0 = 36$  whereas the number of wave frequencies  $N_0$  varies ( $N_0 \approx 550$ – $650$ ) for the individual set of simulations, since a non-equidistant frequency discretisation is used, cf. Eq. (2.21). The cut-off frequency is app. 0.5 Hz. Finally, it should be remembered that the course of the vessel and the wave direction are measured relative to the same datum, that is,  $\beta = \theta$  so that  $\theta = 180^\circ$  is head sea.

Table 1  
Main dimensions of the considered ship

Length, $L_{pp}$	275.0 m
Breadth, $B_{mld}$	40.0 m
Draught, $T$	12.0 m
Displacement	50,000 t

### 3.2. Integrated wave parameters

Basically, the overall outcome of the estimation procedures, being it from the Bayesian Modelling or from the Parametric Modelling, is given by a directional wave spectrum  $E(\omega, \theta)$ . For comparative reasons, integrated wave parameters therefore need to be evaluated in each estimation, and this subsection serves as the reference for the calculation of these parameters. The listed expressions follow from Günther et al. (2006).

The frequency wave spectrum is obtained by integrating the directional wave spectrum with respect to direction

$$F(\omega) = \int E(\omega, \theta) d\theta \quad (3.1)$$

and hence the spectral moment of order  $n$  is defined by

$$m_n = \int \omega^n F(\omega) d\omega. \quad (3.2)$$

Thus, the significant wave height  $H_s$  and the mean wave period  $T_s$  are estimated from

$$H_s = 4\sqrt{m_0}, \quad (3.3)$$

$$T_s = \frac{m_0}{m_1}. \quad (3.4)$$

In addition, the peak period is

$$T_p = \frac{2\pi}{\omega_p}, \quad F(\omega_p) = \max_{\omega} F(\omega). \quad (3.5)$$

The estimated mean wave direction follows from

$$\theta_s = \arctan(d/c), \quad (3.6)$$

where  $d$  and  $c$  are defined according to

$$d = \iint E(\omega, \theta) \sin \theta d\omega d\theta, \\ c = \iint E(\omega, \theta) \cos \theta d\omega d\theta. \quad (3.7)$$

Finally, the mean directional spread is given by

$$\sigma_s = \left( 2 - \frac{2}{m_0} \sqrt{d^2 + c^2} \right)^{0.5} \quad (3.8)$$

which should not be confused with the spreading parameter  $s$ , since the directional spread  $\sigma_s$  is measured in radians.

## 4. Results

### 4.1. Organisation

The overall results of the analyses have been divided into cases corresponding to unimodal spectra and bimodal spectra, and the underlying wave parameters are presented in Tables 3 and 4, respectively. Thus, these tables list the characteristic wave parameters as calculated by the expressions (3.1)–(3.8) and, specifically, the significant wave height  $H_s$ , the peak (wave) period  $T_p$ , the mean

(wave) period  $T_s$ , the mean (wave) direction  $\theta_s$ , and the mean directional spread  $\sigma_s$  are found in the tables. It should be noted that the shape parameter  $\lambda$  of the wave spectrum is not included in the tables, since this parameter is difficult to obtain. A somewhat similar measure could be established by the combined measures of skewness and kurtosis in the spectral description. In the analysis, these numbers are, however, not dealt with.

From the tables, it can be seen that four values, denoted ‘true’, ‘mean’, ‘std’ and ‘error’, are given to each case A, B, . . . , K. The values ‘true’ correspond to the exact parameters of the wave spectrum as seen from Table 2. For the three other values—‘mean’, ‘std’ and ‘error’—two numbers are given to each wave parameter. The first number, i.e. the left one, yields the result as obtained by the Bayesian Modelling, whereas the second number, i.e. the right one, yields the result as obtained by the Parametric Modelling. It is understood that the value ‘mean’ represents the mean value of the specific estimated parameter for the 20 simulations/estimations carried out in the individual cases. The value ‘std’ gives the standard deviation of the parameter based on the 20 estimations and, finally, ‘error’ gives the error between the estimated mean and the true value relative to the true value, except for the parameters related to the wave direction where the absolute value of the error is shown. The two latter values are also based on the mean of the 20 estimations.

In the estimation analysis the wave field is discretised into  $N = 30$  wave frequencies ([0.01–0.30 Hz]) and  $M = 18$  directions ([0–360°]). The sensitivity to discretisation is not studied, but it should be noted that a previous study, Nielsen (2005), indicates that the solution is not particularly sensitive to the values of  $N$  and  $M$  (if chosen appropriately), and in the study it was found that  $N = 30$  and  $M = 18$  are reasonable values to use in the discretisation of the wave field.

### 4.2. Unimodal wave spectra

Table 3 shows the results of Cases A–H. From the table it is seen that both the Bayesian and the Parametric Modelling estimate the energy content of the wave spectra close to the level of the true wave fields. Thus, the mean values of the estimated significant wave height  $H_s$  are, more or less, identical in the individual cases, with the exception of Cases C and E. It is seen that the error on the significant wave height is, in most cases, less than 20% (with the exception of Cases C and E) of the true value, independently of the modelling procedure in question. It should, however, be noted that energy is almost consistently lacking in the estimations. This fact could be due to filtering introduced by the insensitivity of the ship to excitations at certain wave lengths; in particular, short wave lengths since the inertia of the ship is relatively large, cf. Table 1. Indeed, it is seen that the largest errors on the significant wave height are found for Cases A–D which represent wind sea with shorter wave lengths than Cases

Table 3  
True and estimated wave parameters for the unimodal cases

Case		$H_s$ (m)		$T_p$ (s)		$T_s$ (s)		$\theta_s$ (deg.)		$\sigma_s$ (deg.)	
A	true	3.0		8.0		6.6		015		41	
	mean	2.5	2.4	6.8	6.4	7.1	6.2	015	054	43	21
	std	0.2	0.2	0.2	0.4	0.2	0.2	7	10	3	8
	error	-17%	-20%	-15%	-20%	9%	-5%	0	38	2	20
B	true	3.0		8.0		6.6		105		41	
	mean	2.5	2.8	7.9	7.3	7.6	5.9	115	80	59	34
	std	0.1	0.2	0.5	1.6	0.2	0.4	11	13	4	11
	error	-17%	-7%	-1%	-9%	17%	-9%	10	25	18	7
C	true	3.0		8.0		6.6		180		41	
	mean	1.5	2.1	7.3	7.5	7.3	6.8	178	186	23	34
	std	0.6	0.9	0.6	1.2	0.4	0.9	73	58	15	17
	error	-50%	-30%	-9%	-6%	12%	5%	2	6	18	7
D	true	3.0		8.0		6.6		225		41	
	mean	2.2	2.4	8.0	7.2	7.7	5.9	227	264	50	32
	std	0.2	0.3	0.3	1.5	0.1	0.6	9	25	4	14
	error	-27%	-20%	0	-10%	18%	-9%	2	39	9	9
E	true	2.0		14.0		11.0		015		36	
	mean	2.1	2.8	11.7	10.6	10.9	9.6	27	43	30	27
	std	0.2	1.8	1.5	3.4	0.8	2.8	7	33	4	9
	error	5%	40%	-16%	-24%	1%	-13%	12	28	6	12
F	true	2.0		14.0		11.0		105		36	
	mean	2.0	1.9	12.8	13.8	11.1	11.3	109	109	46	33
	std	0.1	0.1	0.7	0.8	0.4	0.6	5	6	4	3
	error	0	-5%	-9%	-1%	1%	3%	4	4	10	3
G	true	2.0		14.0		11.0		180		36	
	mean	1.7	1.7	12.7	13.8	12.1	11.9	182	181	38	38
	std	0.1	0.1	0.5	0.9	0.3	0.7	8	9	3	3
	error	-15%	-15%	-9%	-1%	10%	8%	2	1	2	2
H	true	2.0		14.0		11.0		225		36	
	mean	1.9	1.9	12.9	13.7	11.5	11.2	221	223	44	38
	std	0.1	0.2	0.7	0.9	0.4	0.7	8	10	4	9
	error	-5%	-5%	-8%	-2%	5%	2%	4	2	8	2

Numbers are shown for both the Bayesian (left one) and the Parametric Modelling (right one).

Table 4  
True and estimated wave parameters for the total wave systems of the bimodal cases

Case		$H_s$ (m)		$T_p$ (s)		$T_s$ (s)		$\theta_s$ (deg.)		$\sigma_s$ (deg.)	
I	true	3.6		-		7.5		352		-	
	mean	3.3	3.5	-	-	8.2	6.4	335	292	-	-
	std	0.2	0.4	-	-	0.4	0.6	13	10	-	-
	error	-8%	-3%	-	-	9%	-15%	17	60	-	-
J	true	3.6		-		7.5		195		-	
	mean	2.7	3.0	-	-	9.9	9.0	203	205	-	-
	std	0.1	0.6	-	-	0.3	0.7	6	14	-	-
	error	-25%	-17%	-	-	32%	20%	8	10	-	-
K	true	3.6		-		7.5		105		-	
	mean	3.3	3.7	-	-	8.9	6.6	102	86	-	-
	std	0.2	0.3	-	-	0.2	0.4	9	7	-	-
	error	-8%	3%	-	-	19%	-12%	3	19	-	-

Numbers are shown for both the Bayesian (left one) and the Parametric Modelling (right one).

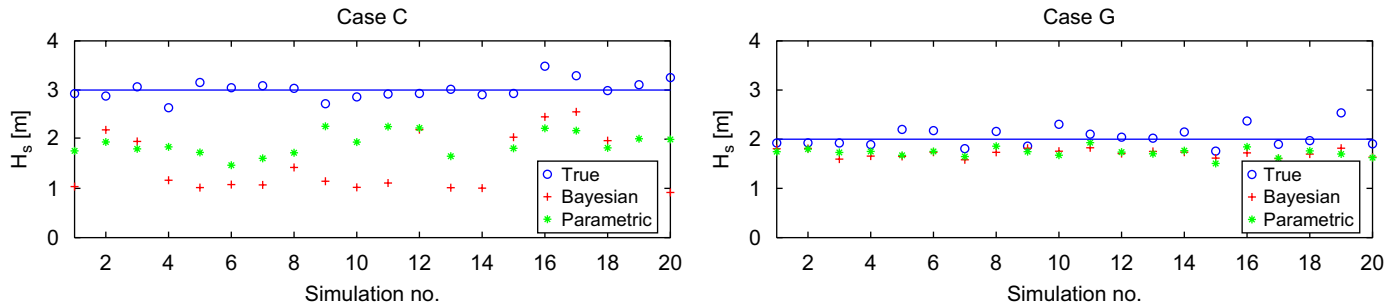


Fig. 1. The significant wave height of Cases C (left) and G (right).

E–H which are characterised as swells. The aspect of filtering explains probably also the apparent peculiarity that the largest error on the estimated significant wave height exists for Case C, which corresponds to head waves ( $\beta = 180^\circ$ ). Thus, the encountered wave system in Case C is the system with the shortest apparent (i.e. encountered) wave lengths relative to the other cases.

With respect to the standard deviation of the significant wave height, the results of the Bayesian as well as the Parametric Modelling are almost constant in all the cases; however, with the smallest standard deviations in the Bayesian Modelling, which means that the Bayesian Modelling produces more stable results. On the other hand, it is observed that the Bayesian results of  $H_s$ , with focus on Cases A–D, exhibit the largest (mean) errors. The reason is likely to be that filtering necessitates a relatively large amount of smoothing introduced by priors. This issue is discussed in more general terms in Nielsen (2005).

Some of the issues concerning the significant wave height are visualised in Fig. 1 which shows the variation of  $H_s$  in the 20 estimations corresponding to Cases C and G. In the figure, the results of the Bayesian and the Parametric Modelling are shown and, in addition, the results of the true wave record for the 20 simulations are visualised. Thus, it is seen that the true significant wave height is not exactly  $H_s = 3.0\text{ m}$  and  $H_s = 2.0\text{ m}$ , respectively, in any of the simulations, which, in principle, ought to be taken into account in the comparisons. Similar plots and results, although not shown and not as bad as Case C, are observed in the remaining cases. As regard to Cases C and G, Fig. 1 evidently illustrates the difference of the wind sea case versus the swell case in respect of the estimated  $H_s$ ; much better estimations are made for the swell case, both in regard to error and standard deviation.

Inherently, the estimated significant wave height gives a measure of the conservation of energy in the estimations. In order to evaluate the correctness of the distribution of energy, polar plots of the contours of the directional wave spectra can be studied. The energy distribution can, however, also be characterised—in a mean sense—by the wave period and the wave direction. Therefore,  $T_p$  and  $T_s$  in combination with  $\theta_s$  and  $\sigma_s$  give a reasonable evaluation of the energy distribution. With due consideration of these numbers, Table 3 shows that the Bayesian Modelling and

the Parametric Modelling exhibit somewhat identical numbers in the individual cases, although it seems that in cases represented by wind sea (Cases A–D), the former method performs the best with respect to the mean wave direction  $\theta_s$ . Thus, it is noted that for the Bayesian Modelling the mean value of the mean wave direction deviates at most  $10^\circ$  from the true mean wave direction, which should be compared to deviations from  $6^\circ$  to  $39^\circ$  for the Parametric Modelling in Cases A–D. For the cases represented by swell (Cases E–H), the estimated mean wave direction is in good agreement with the true value with a slight exception of Case E. Compared to the true numbers, it is seen that the error on the wave period is at most 24%. The aspects of filtering is, however, noted for the wind sea cases, since the peak period  $T_p$  is almost consistently estimated too small, in contrast to the estimated mean period  $T_s$  which, in most cases, has values larger than the true one. Hence, the shape of the frequency wave spectrum, cf. Eq. (3.1), is distorted in the sense that the energy is not distributed in a perfect match with the true distribution of energy. This phenomenon applies to the Bayesian Modelling as well as to the Parametric Modelling and the phenomenon is visualised in Fig. 2 which shows all the estimated frequency wave spectra in the individual wind sea cases (Cases A–D). The results of both the Bayesian Modelling (left plots) and the Parametric Modelling (right plots) are shown. For the Bayesian Modelling it is seen that the energy is distributed within a too short frequency range. In the Parametric Modelling, the problem is of another kind, since it is observed that, in some of the cases, the procedure, frequency-wise, estimates a bimodal spectrum, which means that the spectrum exhibits two peaks. Fig. 3 shows similar plots for Cases E–F which are characterised by swells. From the figure it appears evidently that the best agreement between the estimations and the true spectra are observed for the swell cases. This fact confirms, to some extent, the hypothesis made previously about the aspect of filtering. Hence, due to the relatively large inertia of the considered ship, the vessel is the most sensitive to wave excitations in the lower frequency range, which means that the estimation procedures work the best—for the specific ship—for excitations represented by swells. In summary for the unimodal cases, it can be concluded that the distribution of energy,

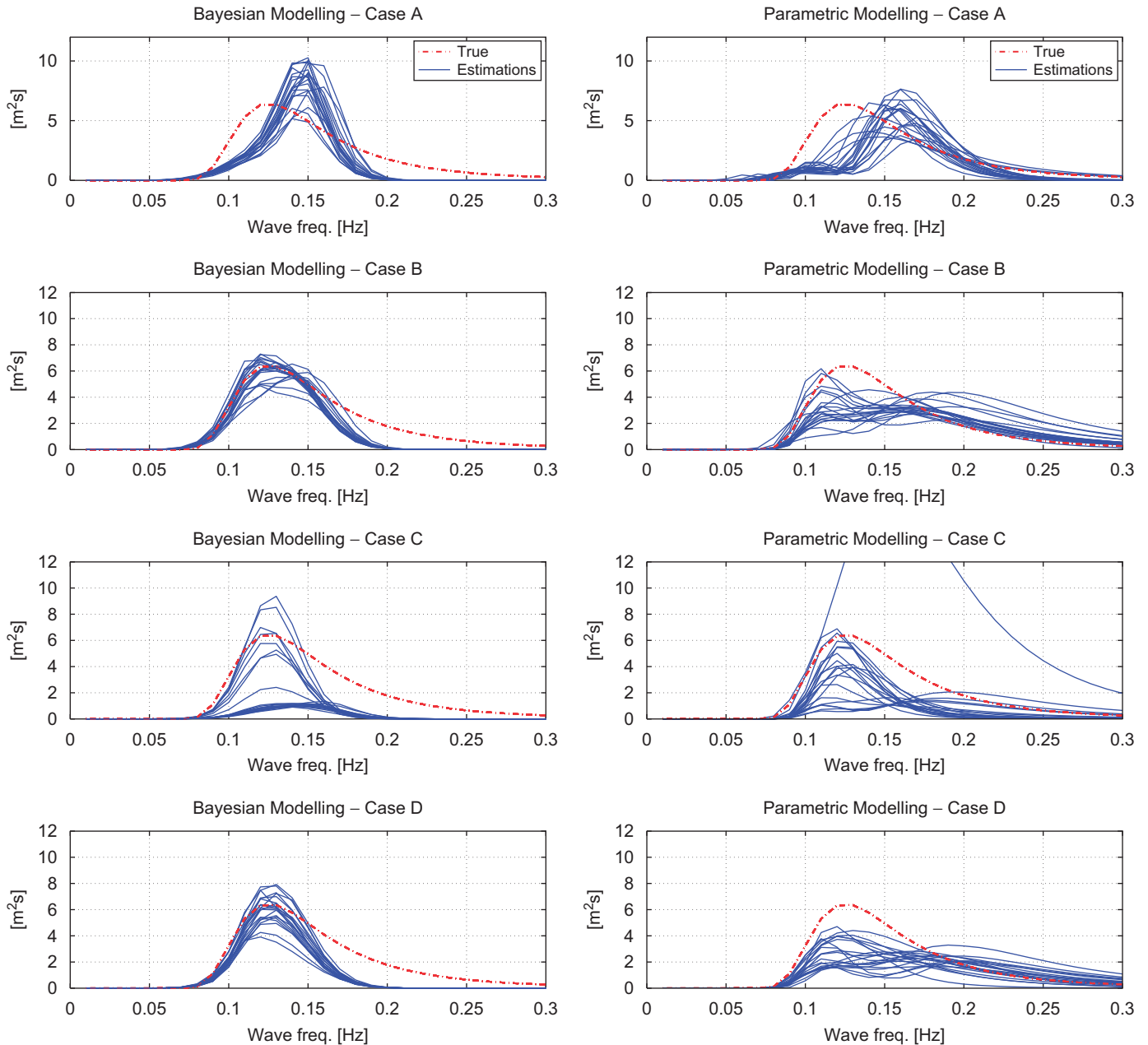


Fig. 2. The estimated frequency wave spectra of Cases A–D (wind sea types).

directional-wise, of the estimated wave spectra is reasonable, independently on the modelling procedure in question although the results of the Bayesian Modelling are more consistent and in line with the true values. The frequency-wise distribution of energy is, however, distorted somewhat for the wind sea cases, whereas there is a good agreement for the swell cases.

As has been mentioned previously, the Bayesian Modelling seems to produce more stable solutions/results compared to the Parametric Modelling. This is seen in terms of the smallest standard deviations on the wave parameters corresponding to the Bayesian Modelling, cf. Table 3, and it is also visualised graphically in Figs. 2

(particularly) and 3. The reason for the instability of the solutions as regard to Parametric Modelling is probably to be found in the search algorithm for the non-linear optimisation problem. In the present study, a gradient based search algorithm is used and when, on the assumption, many local minima exist, the search basin needs to be rather comprehensive/detailed for the algorithm to find the global minimum. The instabilities observed, notably in the wind sea cases, for the Parametric Modelling may therefore be due to problems related to finding local minima instead of a global minimum. This topic does, however, need further studies.

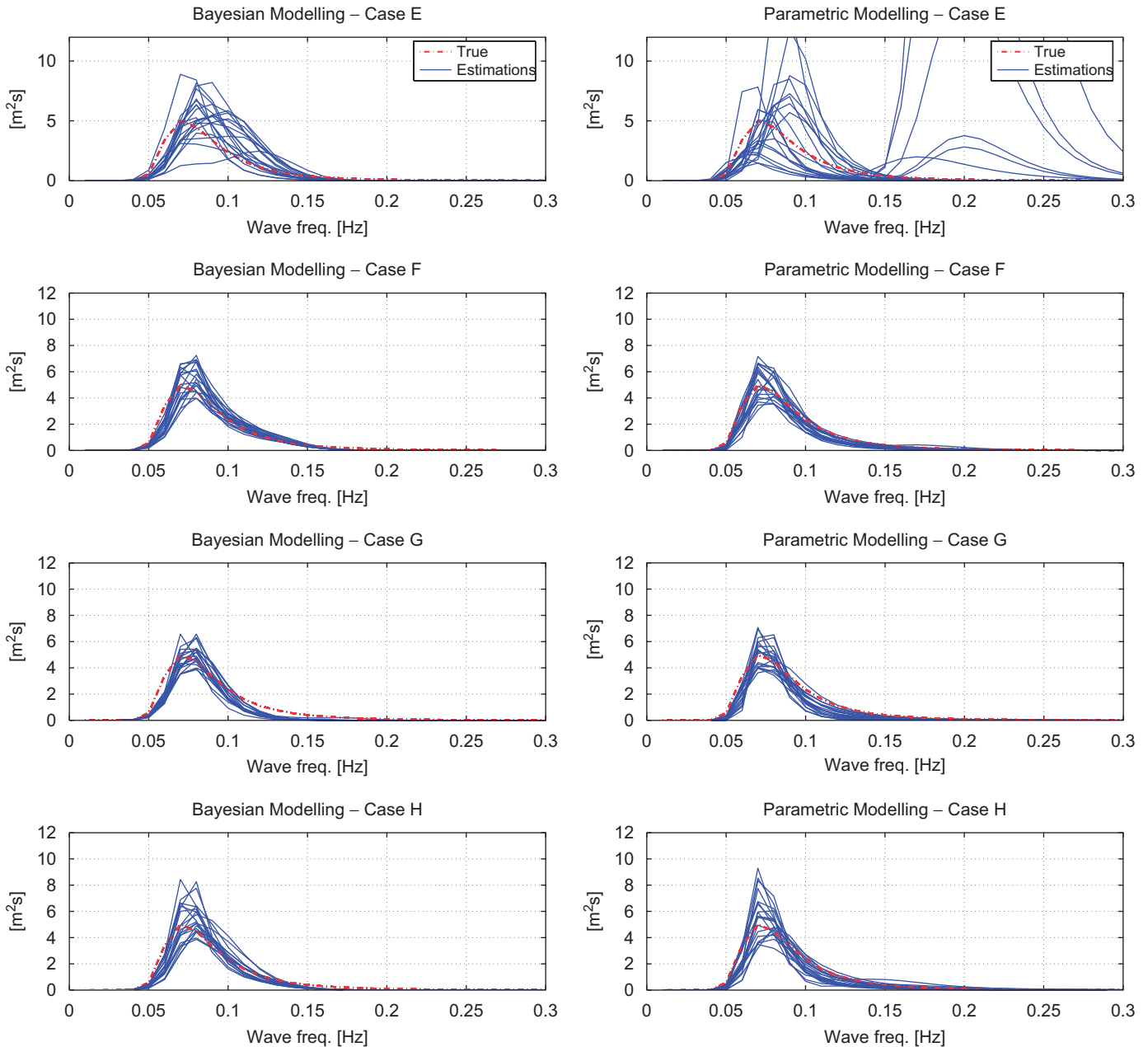


Fig. 3. The estimated frequency wave spectra of Cases E–H (swell types).

#### 4.3. Bimodal wave spectra

Table 4 presents the results corresponding to the bimodal wave spectra, i.e. Cases I–K. It is seen that the table contains results for only the significant wave height  $H_s$ , the mean wave period  $T_s$  and the mean wave direction  $\theta_s$ , since the table represents the total wave system in the individual cases. In addition to Table 4, Table 5 needs therefore to be considered for the partitioning of the wave spectra. Hence, Table 5 shows the estimated mean values of the wave parameters corresponding to the wind sea and the swell components, respectively. The results of the Bayesian (bay) as well as the Parametric (par) Modelling are shown. As regards Table 4, it is seen that, in the mean sense, the

Bayesian Modelling and the Parametric Modelling give reasonable estimates for the significant wave height with the largest error being  $-25\%$  relative to the true value. It is, however, observed that the error on the significant wave height is (almost) consistently to the lower side which means that energy is lacking in the estimations. This phenomenon is similar to that for the unimodal cases and is, probably, explained with the same reason, namely the aspect of filtering. In this respect, it should be noted that the errors on the significant wave height and the mean wave period ( $T_s$ ) of Case J do, indeed, take the largest values. Thus, Case J represents waves with a true mean wave direction ( $\theta_s = 195^\circ$ ) close to head sea which means that the encountered wave system of Case J has the

Table 5  
Partitioning of the bimodal wave spectra

Case		Wind sea					Swell				
		$H_s$ (m)	$T_p$ (s)	$T_s$ (s)	$\theta_s$ (deg.)	$\sigma_s$ (deg.)	$H_s$ (m)	$T_p$ (s)	$T_s$ (s)	$\theta_s$ (deg.)	$\sigma_s$ (deg.)
I	true	3.0	8.0	6.5	015	41	2.0	14.0	11.0	225	36
	bay	2.7	7.4	7.4	004	45	1.9	14.6	14.1	237	31
	par	3.0	6.0	4.6	315	36	1.7	14.0	10.8	232	29
J	true	3.0	8.0	6.5	180	41	2.0	14.0	11.0	225	36
	bay	2.1	10.3	10.2	196	58	1.7	14.2	13.9	241	25
	par	2.7	10.6	8.2	195	34	1.3	14.0	10.8	254	36
K	true	3.0	8.0	6.5	105	41	2.0	14.0	11.0	105	36
	bay	2.8	8.4	8.6	96	47	1.8	12.1	12.7	121	33
	par	2.9	5.9	4.5	100	40	2.3	12.6	9.8	78	29

Mean values from the 20 simulations/estimations are shown for the Bayesian (bay) and the Parametric (par) Modelling in each of the cases.

shortest—encountered—wave lengths compared to the other cases. Hence, due to the relatively large inertia of the vessel, high-frequency components of the wave system are filtered.

With respect to the mean wave direction the Bayesian Modelling yields good estimates for all cases. So does the Parametric Modelling for Cases J and K, but it is seen that the error takes a significant value for Case I. Looking closer into this problem, the inspection of the partitioned wave spectra, see Table 5, reveals that it is the wind sea component that is estimated to the wrong side, by the Parametric Modelling, in the specific case (Case I). Thus, it appears that the wind sea component has a mean value of  $\theta_s = 315^\circ$  for the estimated mean wave direction, which should be compared to a true mean wave direction of  $015^\circ$ . It is difficult to explain this controversy for the Parametric Modelling, since the Bayesian Modelling yields a reasonable mean value ( $004^\circ$ ) for  $\theta_s$  in the 20 estimations of Case I. In addition, it should also be noted that the error by the Parametric Modelling is consistent in the sense that all 20 simulations of Case I give a wrong mean wave direction with a mean standard deviation of  $13^\circ$ . One probable explanation for the error may have to do with the optimisation algorithm which is used in the Parametric Modelling. The method uses a gradient based search algorithm which requires a rather detailed search basin for the initial guesses of the wave parameters, see Nielsen (2006). Hence, by refining the search basin (meaning increased CPU time), the mean wave direction of the wind sea component is estimated to  $\theta_s = 018^\circ$ , which is in good agreement with the true value. This topic will, however, not be discussed any further, but it can be mentioned that it would, most likely, be a better option to use a genetic optimisation algorithm in the Parametric Modelling as discussed by Nielsen (2006) and Pascoal et al. (2005).

With the exception of the estimations by the Parametric Modelling in Case I, Table 5 shows that the distribution of energy, frequency- and directional-wise, is reasonable for the two estimation procedures. Similar plots to Figs. 2 and

3, although not shown, can be produced for Cases I, J and K. Instead of the frequency wave spectra, examples on the estimated directional wave spectra from Cases I, J and K are visualised in Fig. 4 which shows contour plots of the wave spectra in a polar format. It should be pointed out that the figure illustrates only one of the 20 estimated directional wave spectra in each of the cases. In the figure, the true directional spectrum is shown to the left and the results from the Bayesian and the Parametric Modelling are shown in the middle and to the right, respectively. The vessel has a course corresponding to  $0^\circ$ , and the waves are depicted as approaching.

Fig. 4 shows evidently that the Parametric Modelling has a problem with the direction of the wind sea component in Case I; similar plots are observed for all estimations of the Parametric Modelling in the specific case. In this respect, it is important to note that the examples shown—for the Bayesian as well as the Parametric Modelling—are not a special selection of the (best) estimations in the individual cases (I, J and K).

The conclusion on the treatment of the bimodal cases is similar to that given on the unimodal cases. This means that the underlying wave parameters are, in general, captured well by both of the estimation procedures, although the distribution of energy does not match the true distribution completely; in particular energy is lacking in the high-frequency range.

#### 4.4. Bayesian versus Parametric Modelling

The intention of this study is not to make a final, general conclusion on which method is the best to estimate wave spectra from measured ship responses. To draw such a conclusion, much more detailed analyses are needed with respect to type of responses, fields of operation, refinement of the discretisation, type of optimisation algorithm applied by the Parametric Modelling, costs as regards CPU time, etc. However, it is interesting to summarise the results and the discussions made in the preceding in the

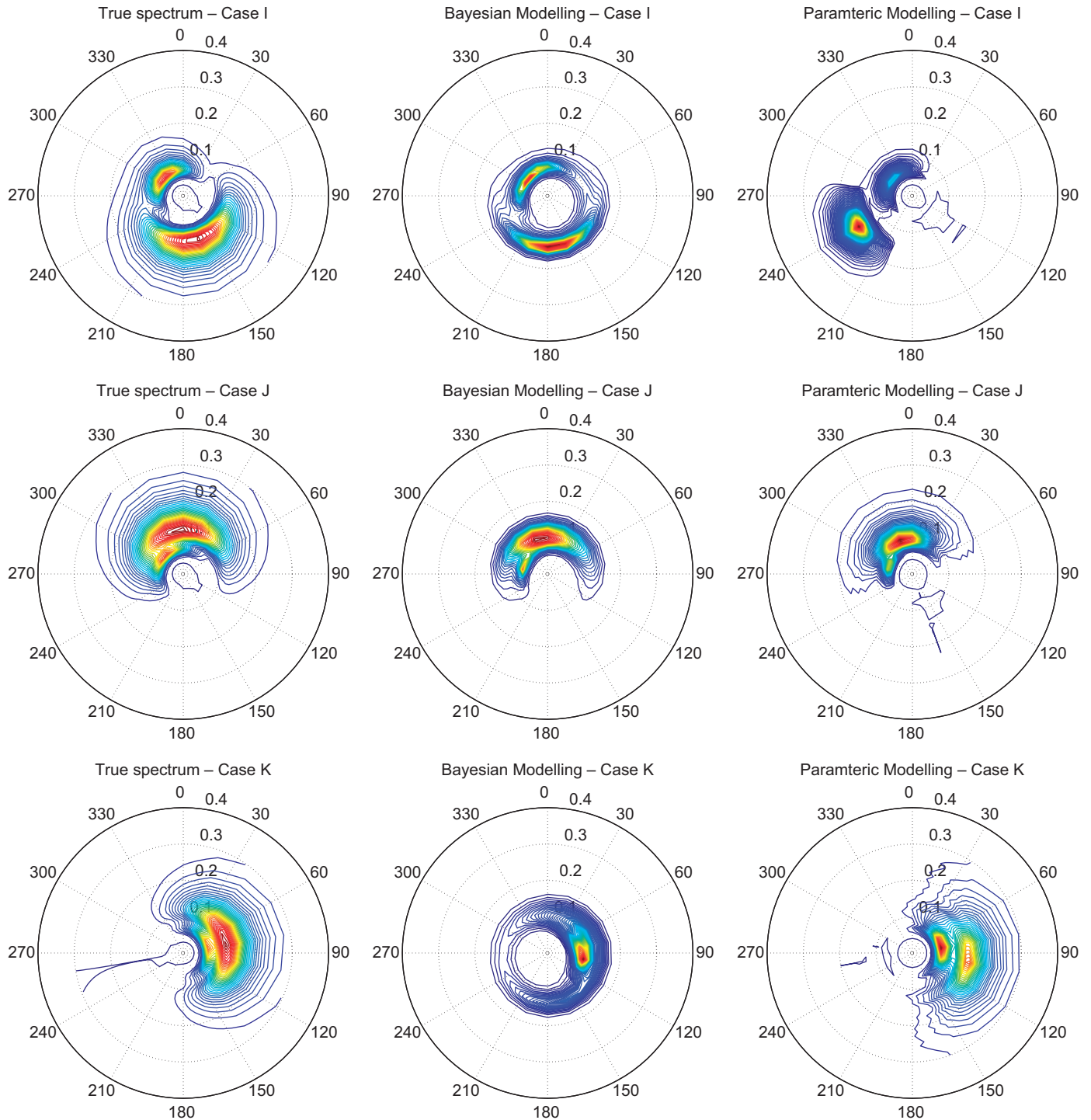


Fig. 4. Examples of contour plots of the estimated directional wave spectra.

form of a graphical visualisation. Fig. 5 shows therefore the errors on the significant wave height, the mean wave period and the mean wave direction, respectively, in all the cases. The figure does not present any new information but it is seen that, in general, the smallest errors are observed for Cases E–H, which are the swell cases. Moreover, the figure illustrates that the Bayesian Modelling seems to be the best procedure to estimate the wave direction. On the other hand, there cannot be made any decisively remarks

concerning  $H_s$  and  $T_s$  from the figure, although the trend of the errors seems to be slightly in favour of Parametric Modelling.

#### 4.5. Responses

The preceding analyses have revealed that the results are influenced by filtering introduced because of the large inertia of a ship. In the specific numerical simulations sway,

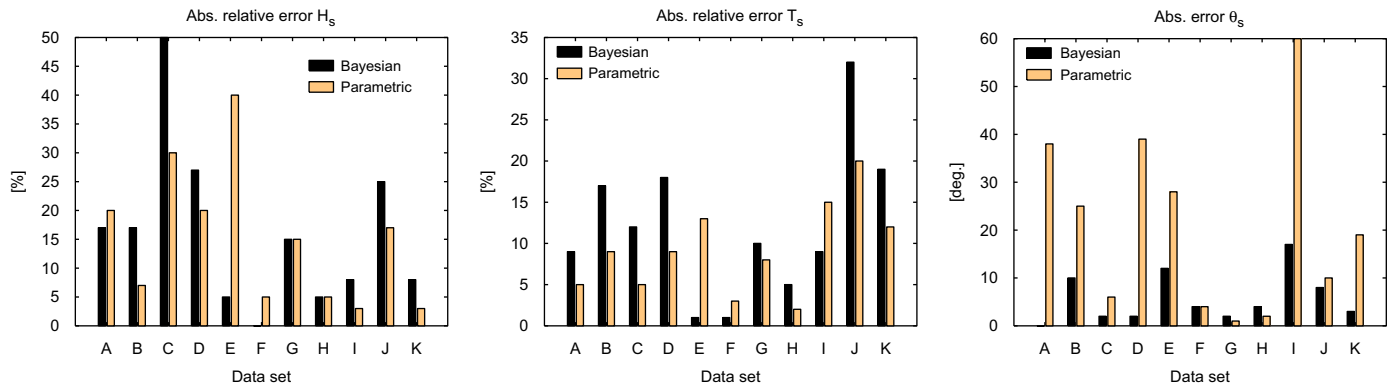


Fig. 5. Visualisation of the errors of the significant wave height (left), the mean wave period (middle) and the mean wave direction (right) in the estimations.

heave and pitch have been considered as the responses, upon which estimations of wave spectra were based. In practical situations there could probably be other kind of responses to make the estimations from. For example, the relative wave height (based on the distance from a fixed point on the ship to the sea surface) could be included as a response, since this type of response has the advantage in not being sensitive to filtering low/high-frequency wave components. Moreover, it is also important to keep in mind that estimation of wave spectra, in the present area of research, is intended for operational decision support to avoid critical events for *the* measured responses. Hence, it may be the case that the introduced filtering will not be of a great importance for the decision support as regards to the specific response(s).

## 5. Conclusions

Two response-based methods for the estimation of wave spectra were studied. Specifically, Bayesian Modelling and Parametric Modelling were applied to estimate directional wave spectra from numerical simulations of motion measurements with the underlying wave parameters known exactly. The considered vessel was a relatively large container ship and, therefore, high-frequency components of the wave excitations were expected to be filtered. From the numerical analyses this phenomenon was, indeed, observed, since the best estimations were made for cases characterised by swells; independently of the estimation procedure. Thus, the results showed that the estimated energy content, represented by the significant wave height, was almost conserved for excitations characterised by wind sea, but the distribution of the energy did not match the true energy distribution perfectly in those cases. For the swell cases this was to a much better extent the case. Based on the present study it can therefore be concluded

- The response-based methods—the Bayesian Modelling and the Parametric Modelling—are capable of estimating sea state parameters from numerical simulations of measured ship responses.
- The energy content is estimated with a reasonable accuracy, but the exact distribution of energy with frequency is difficult to obtain if the measured responses of the vessel are not sensitive to wave excitations in a certain frequency range. That is, filtering influences the results.
- Although filtering influences the results/estimations of the response-based methods it should be remembered that the methods are developed with focus on decision support systems for operational safety of ships. This means that the complete and ‘true’ energy distribution with frequency and direction may not necessarily be important. What is important is the estimation of energy within the frequency range where the ship responds to the excitations.
- As a result of filtering and because of the speed-of-advance problem for an operating ship, wave estimations of response-based methods cannot be expected to be as accurately as the wave estimations of, e.g. a real wave buoy which, on the other hand—in this context—suffers from its fixed position.
- The analyses were carried out for one single vessel speed ( $V = 10$  m/s) only and therefore a sensitivity study as regard to speed remains as a future task in the estimation analysis. However, the case of zero-forward speed has been tested, although not presented, and the results showed no notable—or little favorable—differences.
- Another future task would be to set up the simulations/analyses for a set of responses in which one of the responses does not filter high frequency components of the wave excitations. Thus, it would be interesting to include the relative wave height or a similar measure, e.g. the pressure at a point on the hull under the sea surface, to see if this would improve the wave estimations in the wind sea cases.
- Finally, it is difficult to propose the one estimation procedure—Bayesian Modelling versus Parametric Modelling—in favour of the other, since they perform almost similarly as regards results for the specific analyses. And, in general, the literature also reflects

different opinions about which methodology is the best, e.g. Tannuri et al. (2003) and Pascoal et al. (2005).

## Acknowledgements

The complex-valued frequency response functions have been provided by Det Norske Veritas (DNV) and the author would like to thank Dr. Bo Cerup Simonsen for making the data available. In this regard, the author would like to acknowledge *The Network of Excellence—MAR-STRUCT* for sponsoring a stay at DNV. Moreover, inspiring discussions with Professor Jørgen Juncher Jensen are highly appreciated.

This paper has been carried out as an individual study of WP 2 within the ADOPT project under the Sixth Framework Programme and the financial support is acknowledged.

## References

- Aarnes, J., Krogstad, H., 2001. Partitioning sequences for the dissection of directional ocean wave spectra: a review. Technical report (Paper prepared in the EnviWave research programme).
- Akaike, H., 1980. Likelihood and Bayes procedure. In: Bernardo, J.M., Groot, M.H.D., Lindley, D.U., Smith, A.F.M. (Eds.), *Bayesian Statistics*. University Press, Valencia, pp. 143–166.
- Akaike, H., Nakagawa, T., 1988. *Statistical Analysis and Control of Dynamic Systems*. KTK Scientific Publishers.
- Aschehoug, M., 2003. Scientific paper on the sea state estimation methodology. Technical report, SIREHNA, France (Paper prepared in the HullMon+ project).
- Denis, M.S., Pierson, W., 1953. On the motion of ships in confused seas. *Transactions of SNAME*, vol. 61.
- DNV, 2005. User Manual: WASIM (Technical documentation by DNV).
- Gerling, T., 1992. Partitioning sequences and arrays of directional wave spectra into component wave systems. *Journal of Atmospheric and Oceanic Technology* 9, 111–136.
- Goda, Y., 2000. *Random Seas and Design of Maritime Structures*, Advanced Series on Ocean Engineering, vol. 15. World Scientific, Singapore.
- Günther, H., Dannenberg, J., Kluwe, F., 2006. Relevant quantities for environmental modelling including adequate quality criteria. Technical report, GKSS (Paper prepared in the ADOPT project).
- Hogben, N., Cobb, F., 1986. Parametric modelling of directional wave spectra. In: *Proceedings of 18th Offshore Technology Conference*, Houston, Texas, pp. 489–498.
- Huss, M., Olander, A., 1994. Theoretical seakeeping predictions on board ships—a system for operational guidance and real time surveillance. Technical report, Naval Architecture, Department of Vehicle Engineering, Royal Institute of Technology.
- Iseki, T., Ohtsu, K., 2000. Bayesian estimation of directional wave spectra based on ship motions. *Control Engineering Practice* 8, 215–219.
- Iseki, T., Terada, D., 2002. Bayesian estimation of directional wave spectra for ship guidance systems. *International Journal of Offshore and Polar Engineering* 12, 25–30.
- Jensen, J., Capul, J., 2006. Extreme response predictions for jack-up units in second order stochastic waves by FORM. *Probabilistic Engineering Mechanics* 21 (4), 330–338.
- Jensen, J., Pedersen, P., 2006. Critical wave episodes for assessment of parametric roll. In: *Proceedings of IMDC'06*, Ann Arbor, USA.
- Komen, G., Cavaleri, L., Donelan, M., Hasselmann, K., Hasselmann, S., Janssen, P., 1994. *Dynamics and Modelling of Ocean Waves*. Cambridge University Press, Cambridge, MA.
- Longuet-Higgins, M., Cartwright, D., Smith, N., 1961. Observations of the directional spectrum of sea waves using the motions of a floating buoy. *Ocean Wave Spectra*, 111–136.
- Neumaier, A., Schneider, T., 2001. Estimation of parameters and eigenmodes of multivariate autoregressive models. *ACM Transactions on Mathematical Software* 27 (1), 27–57.
- Nielsen, J., 2004. SeaSense—Slut Rapport. Technical report, Force Technology (Report on the joint project SeaSense. The report is in Danish).
- Nielsen, U., 2005. Estimation of directional wave spectra from measured ship responses. Ph.D. Thesis, Section of Coastal, Maritime and Structural Engineering, Department of Mechanical Engineering, Technical University of Denmark.
- Nielsen, U., 2006. Estimations of on-site directional wave spectra from measured ship responses. *Marine Structures* 19 (1), 33–69.
- Nielsen, U., 2007. Introducing two hyperparameters in Bayesian estimation of wave spectra (Probabilistic Engineering Mechanics, under review).
- Pascoal, R., Soares, C., Sørensen, A., 2005. Ocean wave spectral estimation using vessel wave frequency motions. In: *Proceedings of OMAE2005*, Halkidiki, Greece.
- Press, W., Flannery, B., Teukolsky, S., Vetterling, W., 1992. *Numerical Recipes in FORTRAN77: The Art of Scientific Computing*, second ed. Cambridge University Press, Cambridge, MA.
- Tannuri, E., Sparano, J., Simos, A., Cruz, J.D., 2003. Estimating directional wave spectrum based on stationary ship motion measurements. *Applied Ocean Research* 25, 243–261.
- Waal, O., Aalbers, A., Pinkster, J., 2002. Maximum likelihood method as a means to estimate the directional wave spectrum and the mean wave drift force on a dynamically positioned vessel. In: *Proceedings of OMAE2002*, Oslo, Norway.